NANO LETTERS

Letter

pubs.acs.org/NanoLett

Tuning the Outward to Inward Swelling in Lithiated Silicon Nanotubes via Surface Oxide Coating

Jiangwei Wang,[*,†,‡,▽] Hao Luo,[§,▽] Yang Liu,[∥,▽] Yang He,[‡] Feifei Fan,[⊥] Ze Zhang,[†] Scott X. Mao,[*,‡] Chongmin Wang,[*,#] and Ting Zhu[§]

[†]Center of Electron Microscopy and State Key Laboratory of Silicon Materials, School of Materials Science and Engineering, Zhejiang University, Hangzhou 310027, China

[‡]Department of Mechanical Engineering and Materials Science, University of Pittsburgh, Pittsburgh, Pennsylvania 15261, United States

[§]Woodruff School of Mechanical Engineering, Georgia Institute of Technology, Atlanta, Georgia 30332, United States

[∥]Department of Materials Science and Engineering, North Carolina State University, Raleigh, North Carolina 27695, United States

[⊥]Department of Mechanical Engineering, University of Nevada, Reno, Nevada 89557, United States

[#]Environmental Molecular Sciences Laboratory, Pacific Northwest National Laboratory, Richland, Washington 99352, United States

Supporting Information

ABSTRACT: Electrochemically induced mechanical degradation hinders the application of Si anodes in advanced lithium-ion batteries. Hollow structures and surface coatings have been often used to mitigate the degradation of Si-based anodes. However, the structural change and degradation mechanism during lithiation/delithiation of hollow Si structures with coatings remain unclear. Here, we combine in situ TEM experiment and chemomechanical modeling to study the electrochemically induced swelling of amorphous-Si (*a*-Si) nanotubes with different thicknesses of surface SiO_x layers. Surprisingly, we find that no inward expansion occurs at the inner surface during lithiation of *a*-Si nanotubes with native oxides. In contrast, inward expansion can be induced by increasing the thickness of SiO_x on the outer surface, thus reducing the overall outward swelling of the lithiated nanotube. Moreover, both the sandwich lithiation mechanism and the two-stage lithiation process in *a*-Si nanotubes remain unchanged with the increasing thickness of surface coatings. Our chemomechanical modeling reveals the mechanical confinement effects in lithiated *a*-Si nanotubes with and without SiO_x coatings. This work not only provides insights into the degradation of nanotube anodes with surface coatings but also sheds light onto the optimal design of hollow anodes for high-performance lithium-ion batteries.

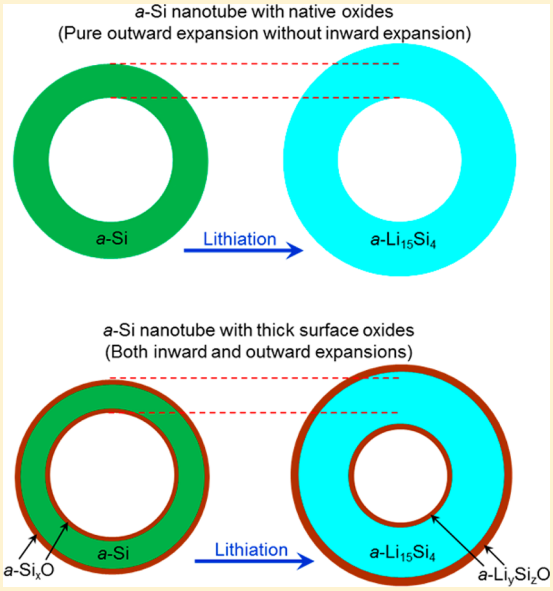

KEYWORDS: *Nanotube, lithium-ion batteries, in situ TEM electrochemical testing, surface coating, volume expansion, mechanical confinement*

Recent development of portable electronics and electric vehicles requires advanced lithium-ion batteries (LIBs) with high energy density and long cycle stability. Among the various anode materials for LIBs, silicon (Si) is a promising candidate, due to the highest theoretical capacity of 3579 mAh/g ($Li_{15}Si_4$) at room temperature.[1,2] However, one serious drawback of Si anodes is the large volume changes (up to ~270%) during charge and discharge cycling.[1,2] Such large volume changes often cause the fracture of both Si[2−4] and solid electrolyte interphases (SEIs),[1,5] resulting in electrically disconnected components and capacity fade. In addition, new SEIs grow on the fresh surface of fractured Si, consuming active Li ions and contributing to capacity fade.[6,7]

During the past few years, considerable efforts have been made to mitigate the mechanical degradation of Si anodes by using nanostructures,[8−10] nanocomposites,[11−14] and surface coatings.[9,15−22] In these engineered Si anodes, open space or flexible matrix (e.g., carbon nanofiber) was introduced to accommodate the lithiation-induced large volume changes.[8−12] Surface coatings (e.g., SiO_2,[9,16−21] Al_2O_3,[22] TiO_2,[22,23] and carbon[13,15,24]) were also often applied to alleviate the

Received: June 22, 2016
Revised: August 10, 2016
Published: August 18, 2016

DOI: 10.1021/acs.nanolett.6b02581
Nano Lett. 2016, 16, 5815−5822

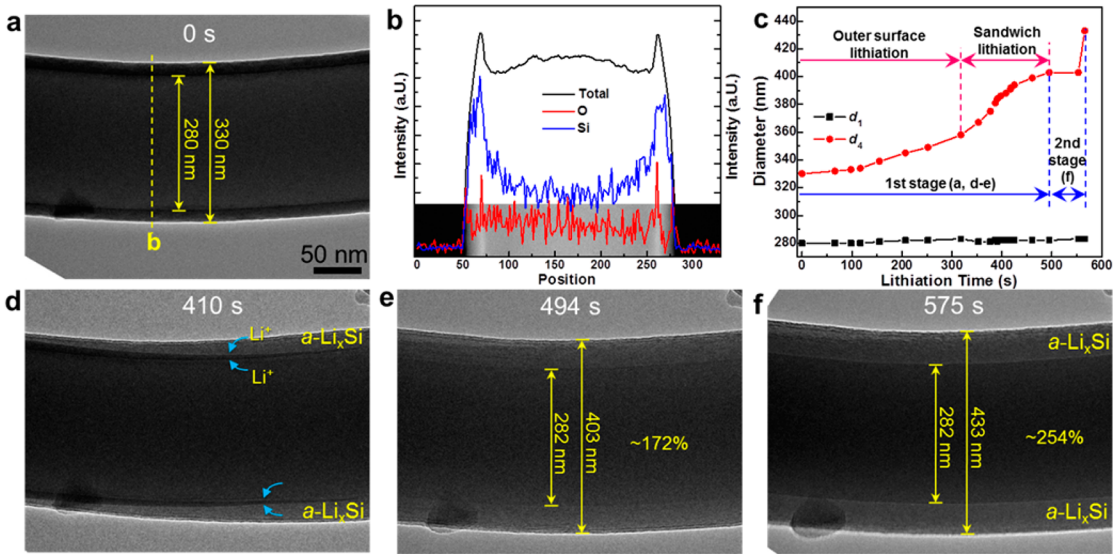

Figure 1. First lithiation of an *a*-Si nanotube with native oxide. (a) Pristine *a*-Si nanotube with native oxide; the inner (d_1) and outer (d_4) diameters of this nanotube are 330 and 280 nm, respectively. (b) EDS line scanning profile showing the element distributions along the radial direction of *a*-Si nanotube. The native oxide layers on both the inner and outer surfaces are less than 2 nm. (c) Change of d_1 and d_4 as a function of lithiation time. (d–f) Time-lapse images of lithiation of the *a*-Si nanotube with native oxide, showing a two-stage process. In the first-stage, lithiation first initiated from the outer surface (denoted as outer surface lithiation), and then started from the inner surface, yielding a sandwich structure of *a*-Li_xSi/*a*-Si/*a*-Li_xSi (panel d, denoted as sandwich lithiation). The first-stage lithiation finished when the sandwich structure disappeared (e). In the second stage, d_4 kept unchanged until a sudden increase; while d_1 did not change during the whole lithiation process.

mechanical degradation and/or improve the conductivity and surface stability of Si anodes. Recently, Si-based anodes with hollow structures, including nanotubes,[9,19] porous nanowires, and nanoparticles,[8,25,26] have attracted great interests in the development of high-performance LIBs. The free space inside these hollow structures is expected to accommodate the volume change and thus reduce the outward expansion, thereby mitigating the degradation of both Si nanostructures and SEIs. However, the actual morphological changes and degradation of these hollow Si nanostructures during electrochemical cycling remain largely unexplored. On the other hand, surface coatings have been widely applied to hollow Si nanostructures for constraining the volume expansion and/or serving as artificial SEIs.[9,22] Among the various coatings, silicon oxide (SiO_x) has gained considerable attention for Si-based anodes due to easy processing via thermal treatment.[9,16−21] In principle, the SiO_x coating can mechanically confine the outward expansion of Si-based hollow structures and reduce the fracture of SEIs, leading to improved battery performance.[9,19] However, it is still unclear to what degree the swelling of Si-based hollow nanostructures can be confined by the surface SiO_x layers and whether or not the lithiation mechanism of Si nanostructures remain unchanged with the application of surface coatings. To address these questions, the amorphous Si (*a*-Si) nanotubes with surface SiO_x layers represent a clean system to study the effect of SiO_x coatings.

In this work, we perform an in situ TEM study on the electrochemically induced swelling behavior of individual *a*-Si nanotubes with different thicknesses of surface SiO_x layers. Our in situ TEM experiment allows for not only direct observation of the real-time lithiation process, but also precise measurement (with the nanometer resolution) of the geometrical changes during lithiation of *a*-Si nanotubes. Surprisingly, we find that no inward expansion occurred at the inner surface after the full lithiation of *a*-Si nanotubes with native oxides. Moreover, we show that increasing the thickness of SiO_x at the *outer* surface can facilitate the mechanical confinement on the lithiated *a*-Si nanotubes, causing an inward expansion. In contrast, SiO_x coating on the *inner* surface can serve as a mechanical barrier to hinder the inward expansion. Furthermore, we observe that the sandwich lithiation mechanism and two-stage lithiation process of *a*-Si nanotubes remained unchanged with the increasing thickness of surface coatings. In addition, our chemomechanical modeling provides insights into the mechanical confinement of SiO_x coatings in lithiated *a*-Si nanotubes, underscoring the critical role of anisotropy of lithiation-induced chemical strains.

Figure 1 shows the electrochemical lithiation of an *a*-Si nanotube with native oxides. Prior to lithiation, the inner diameter (d_1) and outer diameter (d_4) of the *a*-Si nanotube were 280 and 330 nm, respectively (Figure 1a). The energy dispersive spectroscopy (EDS) line scanning profile showed that both the inner and outer surfaces were covered with a thin layer of native oxide, with the thickness less than 2 nm (Figure 1b). By applying a −3 V potential, lithiation first initiated from the outer surface and proceeded radially by inward movement of a sharp interface, which separated the dark *a*-Si reactant with the light-gray amorphous Li_xSi (*a*-Li_xSi) product. This indicates the operation of a two-phase mechanism of lithiation.[27] After a while, lithiation also started from the inner surface and proceeded radially by outward movement of a two-phase boundary (Figure 1d). As a result, *a*-Li_xSi alloys formed on both the outer and inner surfaces, yielding a sandwich structure of *a*-Li_xSi/*a*-Si/*a*-Li_xSi (Figure 1d). This is consistent with the sandwich lithiation in an *a*-Si layer coated on a carbon nanofiber.[11] It is also noted that the lithiation of *a*-Si nanotubes is a two-stage process.[27] That is, after the first-stage sandwich lithiation completely consumed the *a*-Si layer, the resulting volume expansion of the tube wall was only ∼172% (Figure 1e). This suggests the formation of an intermediate *a*-Li_xSi phase with $x \approx 2.3$, which was estimated from a linear relationship between the volume expansion and the Li content

DOI: 10.1021/acs.nanolett.6b02581
Nano Lett. 2016, 16, 5815−5822

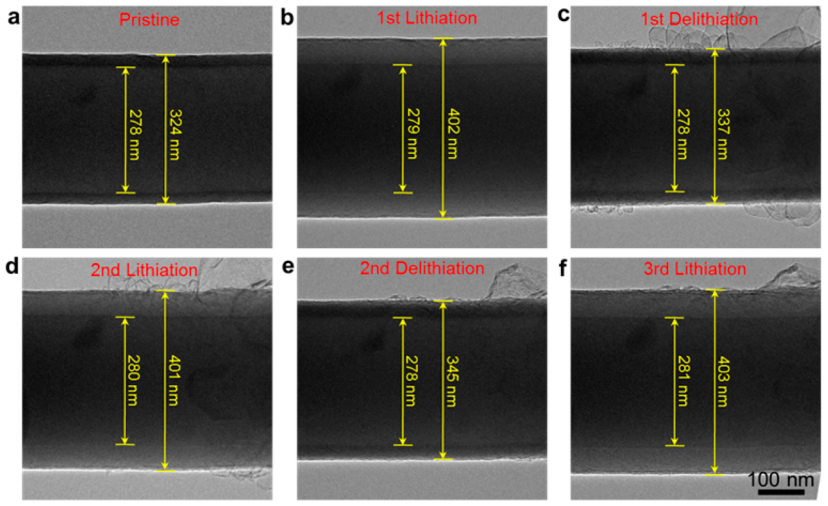

Figure 2. Structural evolution in lithiation−delithiation cycling of an *a*-Si nanotube with native oxides (different from the nanotube in Figure 1). (a) Pristine nanotube. (b−f) Reversible volumetric changes occurred during three lithiation−delithiation cycles, without any inward expansion at the inner surface of the nanotube.

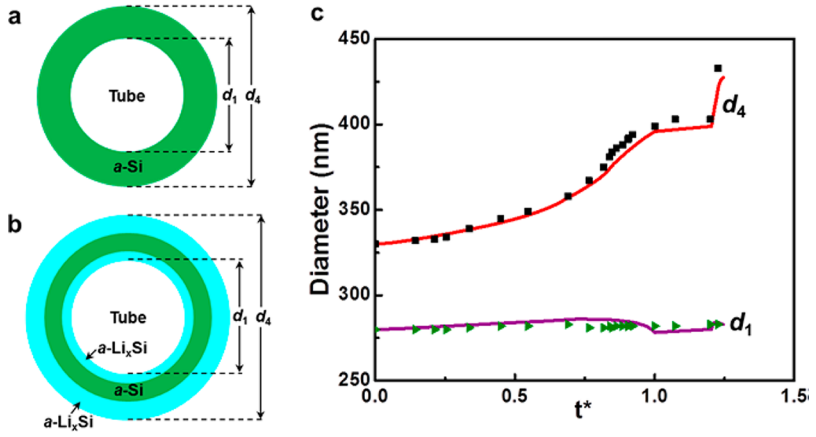

Figure 3. Chemomechanical modeling of the lithiation dynamics in an *a*-Si nanotube with native oxide. (a) Schematic of the model representing the cross section of an *a*-Si nanotube before lithiation. (b) Schematic of formation of a sandwich structure of *a*-Li_xSi/*a*-Si/*a*-Li_xSi during the first-stage lithiation. (c) Comparison between the experimental and simulation results of d_1 and d_4 as a function of reduced time t^* during the two-stage lithiation. The reduced time t^* is defined as the lithiation time normalized by the duration of the first-stage lithiation.

(x) in Li_xSi alloys.[28,29] During the second-stage lithiation, *a*-Li_xSi was further lithiated without a visible interface. This indicates the operation of a possible single-phase mechanism of lithiation with a smooth and gradual change of Li concentration. At the end of the second-stage lithiation, d_1 and d_4 became 282 and 433 nm, respectively (Figure 1f). The corresponding volume expansion in the tube wall (relative to *a*-Si) was ∼254%, close to the theoretical value (∼270%) for the $Li_{15}Si_4$ phase. The apparent outward expansion of this nanotube (i.e., increase of d_4 after full lithiation) is ∼31%. Figure 1c shows d_1 and d_4 as a function of lithiation time, which further corroborates the two-stage lithiation in *a*-Si. It is seen that, during the first-stage lithiation, the outer diameter d_4 increased significantly, while the inner diameter d_1 remained nearly constant. During the second-stage lithiation, d_4 kept unchanged for a short time and then increased quickly from 403 to 433 nm; meanwhile, d_1 still remained nearly constant. The two-stage lithiation of *a*-Si has been previously shown to have a significant impact on the morphological changes in lithiated *a*-Si electrodes.[27] In this work, we further study the effects of oxide thickness on the lithiation behavior of *a*-Si nanotubes.

The lack of inward expansion at the inner surface is unexpected during the sandwich lithiation of *a*-Si nanotubes. This is because once lithiation started from the inner surface, both the lithiation product of *a*-$Li_{2.3}Si$ near the outer surface and the unlithiated *a*-Si in the midlayer would mechanically confine the lithiation-induced volume expansion near the inner surface, and accordingly inward expansion was expected to occur to some degree. However, in eight *a*-Si nanotube samples studied in this work, no inward expansion was observed during the whole lithiation process. Moreover, the lack of inward expansion was also observed upon electrochemical cycling of *a*-Si nanotubes that produced reversible volumetric changes. As shown in Figure 2, no inward expansion occurred during the first three cycles of lithiation−delithiation of an *a*-Si nanotube with native oxides. Besides, significant volume expansions were also observed after the lithiation of Si anodes with other types of hollow structures, such as porous Si nanowire and nanoparticle (Figure S1).

To understand the origin of lack of inward expansion at the inner surface of lithiated *a*-Si nanotubes, we developed a chemomechanical model to simulate the two-stage lithiation

DOI: 10.1021/acs.nanolett.6b02581
Nano Lett. 2016, 16, 5815−5822

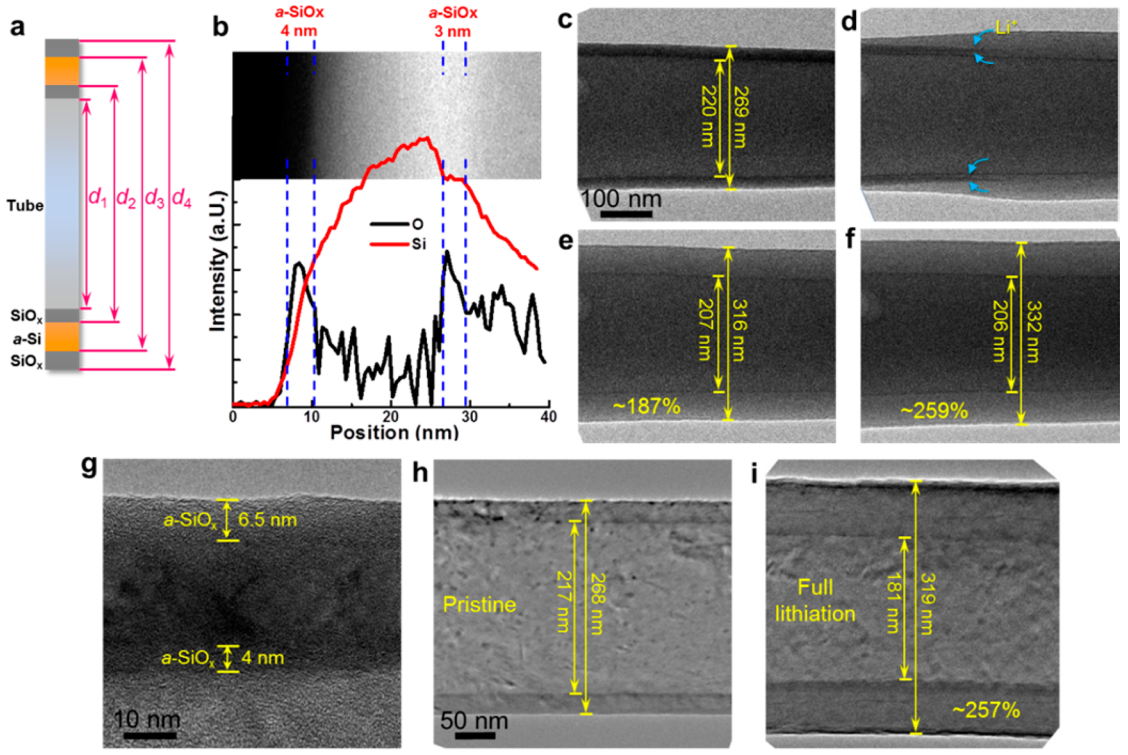

Figure 4. Lithiation of two *a*-Si nanotubes with different thicknesses of oxide coatings. (a) Schematic of the four diameters of d_1, d_2, d_3, and d_4 in an SiO_x/Si/SiO_x nanotube before lithiation, corresponding to the inner surface, the interface between the inner SiO_x and *a*-Si layers, the interface between the outer SiO_x and *a*-Si layers, and the outer surface, respectively. (b–f) Lithiation of an *a*-Si nanotube with 3 and 4 nm SiO_x on the inner and outer surfaces, respectively (denoted as 3‖4 nm SiO_x/Si/SiO_x nanotube). (b) EDS line scanning profile showing the thicknesses of the inner and outer SiO_x layers. (c–f) Time-lapse TEM images of lithiation. It is seen from (d) that lithiation initiated first from the outer surface and then from the inner surface, leading to a sandwich lithiation structure. (g–i) Lithiation of an *a*-Si nanotube with 4 and 6.5 nm SiO_x on the inner and outer surfaces, respectively (denoted as 4‖6.5 nm SiO_x/Si/SiO_x nanotube). (g) High-resolution TEM (HRTEM) image showing the thicknesses of the inner and outer SiO_x layers. (h–i) TEM images before and after lithiation.

process in an *a*-Si nanotube (see the Supporting Information). Our model accounts for the sandwich two-phase lithiation during the first stage and the single-phase lithiation during the second stage. Figure 3a shows the setup of our 2D model representing the cross section of an *a*-Si nanotube before lithiation. To reveal the dominant physical effects of lithiation-induced volume expansion, we neglected the thin layers of native oxides on the inner and outer surfaces of the nanotube. Figure 3b presents a schematic illustration of our model during the first-stage lithiation via a sandwich two-phase process. In addition, the plane-strain condition was imposed in our simulations, on the basis of TEM observation of negligible axial elongation during the entire lithiation process, which has been previously reported for lithiation of both crystalline and amorphous Si nanowires/nanotubes.[5]

Figure 3c shows the simulation results of geometrical changes (solid lines) in a lithiated *a*-Si nanotube as a function of reduced time (t^*), which are in close agreement with the experimental measurements (symbols). Figure S2 shows the associated simulation results of spatial distributions of Li and stresses after lithiation starts at the inner surface. These chemomechanical simulation results provide insights into the origin of lack of inward expansion at the inner surface of the lithiated *a*-Si nanotube. That is, the anisotropy of lithiation-induced chemical strains critically controls the geometrical changes in lithiated *a*-Si nanotubes; the values of anisotropic chemical strains used in our simulations are given in the Supporting Information. While one tends to intuitively assign the isotropic volume expansion (with the associated isotropic chemical strain coefficients β_{ij}) to a lithiation process for *a*-Si, the geometrical constraints within the tube cross section on lithiation cause symmetry breaking in the radial and hoop directions of the nanotube, thereby resulting in a strong anisotropy in the chemical strains of lithiation.[30] As shown by Hsueh and Evans,[31] Huang et al.,[32] and Liang et al.,[33] the degree of anisotropy of chemical strains dictates the resulting elastic–plastic deformation, particularly regarding the outward versus inward radial displacement in a structure with the curved geometry such as a cylindrical wire or spherical particle. Importantly, the chemical strains with a large hoop component tend to produce a large outward radial displacement at the inner surface of the nanotube, owing to the larger perimeter in the hoop direction at the larger radial distance. This tendency of outward expansion competes with that of inward expansion caused by the hindrance effects from both the lithiation product of *a*-$Li_{2.3}Si$ near the outer surface and the unlithiated *a*-Si in the midlayer. In our numerical study, we found that the chemical strains should be chosen appropriately in an anisotropic manner (as discussed in the Supporting Information), so that the model is sufficiently robust to produce a negligibly small displacement at the inner surface for both the first stage of two-phase lithiation and the second stage of single-phase lithiation. That is, we chose a finite hoop chemical strain to avoid the inward expansion of the inner surface arising from the mechanical confinement due to both the lithiation product of *a*-$Li_{2.3}Si$ near the outer surface and the unlithiated *a*-Si in the

DOI: 10.1021/acs.nanolett.6b02581
Nano Lett. 2016, 16, 5815–5822

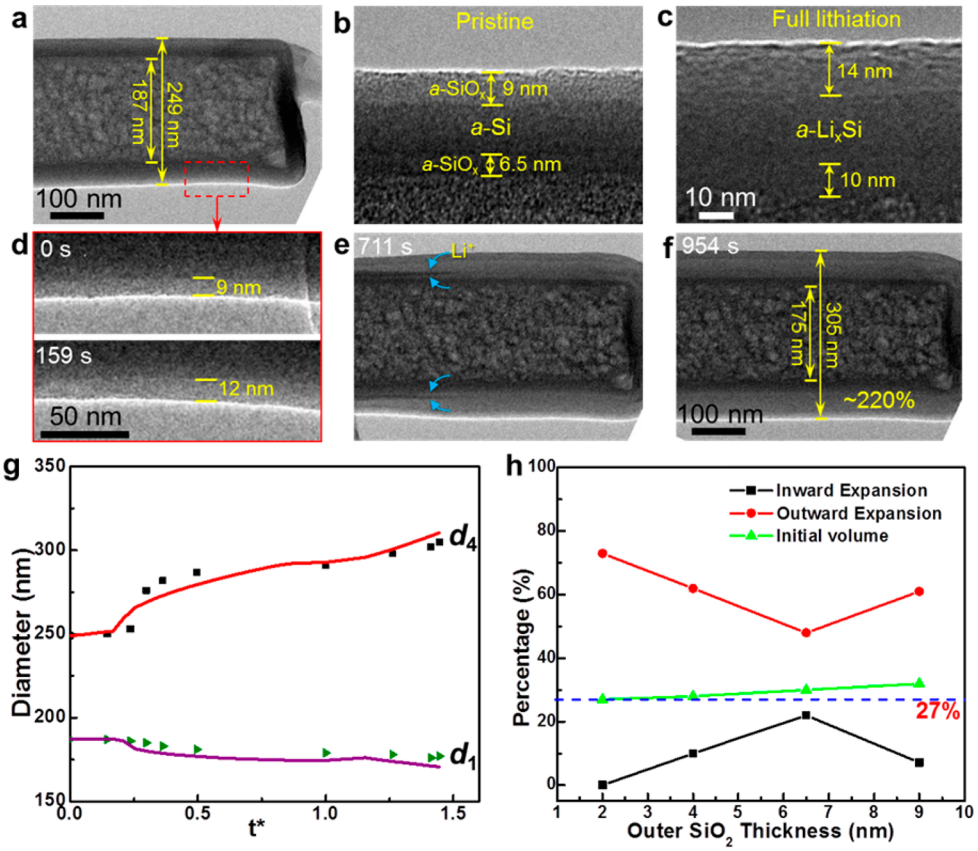

Figure 5. Lithiation of a 6.5‖9 nm SiO_x/Si/SiO_x nanotube and mechanical confinement effects of the outer SiO_x layers on lithiated *a*-Si nanotubes. (a) Pristine 6.5‖9 nm SiO_x/Si/SiO_x nanotube. (b–c) HRTEM image showing the thickness of the inner and outer SiO_x layers before (b) and after (c) lithiation. (d) The outer SiO_x layer was first lithiated, accompanied by a thickness increase from 9 to 12 nm. (e–f) TEM images showing the first-stage lithiation, resulting in a sandwich lithiation structure, and the second-stage lithiation, resulting in a total volume expansion of ∼220% (relative to *a*-Si). (g) Comparison between the experimental and simulation results of d_1 and d_4 as a function of reduced time t^* during the two-stage lithiation of the 6.5‖9 nm SiO_x/Si/SiO_x nanotube. (h) Experimental results showing the percentage contributions of inward and outward volume expansions to the total volume expansion of the fully lithiated *a*-Li_xSi alloy in *a*-Si nanotubes with different thicknesses of the outer SiO_x layers.

midlayer. However, this hoop chemical strain cannot be large enough to cause a pronounced outward expansion of the inner surface. Hence, our chemomechanical simulations suggest that the lack of inward expansion at the inner surface of lithiated *a*-Si nanotubes with native oxides can be attributed to a balance between two competing effects: one is the driving force arising from the anisotropic chemical strains of lithiation in a curved nanotube and the other is the hindrance of other lithiated and unlithiated parts in the system. We note that the chemomechanical model employed in this work does not resolve a more fundamental question regarding how the degree of anisotropy of chemical strains is physically determined when the lithiation reaction predominantly occurs at the sharp phase boundary. A more physically based chemomechanical model is needed for a deeper understanding of this issue in the future.

We next studied the effect of mechanical confinement from thick oxides, in order to examine to what extent the geometrical changes and particularly the lithiation-induced swelling at the outer surface of the nanotube can be confined by coatings. In our experiments, the thickness of SiO_x layers was controlled via thermal treatment of *a*-Si nanotubes in atmosphere for different durations. In order to clearly characterize the geometry of nanotubes with inner and outer oxide coatings, we define the diameters of d_1, d_2, d_3, and d_4 (Figure 4a), which respectively correspond to the inner surface, the interface between the inner SiO_x and *a*-Si layers, the interface between the outer SiO_x and *a*-Si layers, and the outer surface. Figure 4b–f shows the lithiation behavior of an *a*-Si nanotube with 3 and 4 nm SiO_x on its inner and outer surfaces, respectively (Figure 4b, denoted as 3‖4 nm SiO_x/Si/SiO_x nanotube). Note that the inner surface layer of SiO_x is slightly thinner than the outer surface layer. This could be attributed to the larger hoop compression in the inner layer induced by oxidation than in the outer layer, causing the slower oxidation kinetics in the former. Figure 4c–f shows the lithiation process of the 3‖4 nm SiO_x/Si/SiO_x nanotube. Before lithiation, the four diameters were 220, 226, 261, and 269 nm, respectively. Lithiation first initiated from the outer surface and then started from the inner surface, leading to a sandwich structure (Figure 4d), in consistent with the nanotube with native oxides (Figure 1). Moreover, lithiation of this 3‖4 nm nanotube also proceeded by a two-stage process, as shown by Figure 4c–f as well as by changes of d_1 and d_4 as a function of lithiation time in Figure S3. After the first-stage lithiation, d_1, d_2, d_3, and d_4 changed to 207, 213, 307, and 316 nm, respectively, corresponding to a volume expansion of ∼187% in the *a*-Si layer (Figure 4e). After the second-stage lithiation, the four diameters further changed to 204, 212, 323, and 332 nm, respectively, giving a total volume expansion of ∼259% in the *a*-Si layer (Figure 4f). It is interesting to note that a marked inward expansion occurred at the inner surface during the lithiation of this 3‖4 nm nanotube, as manifested by the change of d_2 from 226 nm before lithiation to 212 nm after full

DOI: 10.1021/acs.nanolett.6b02581
Nano Lett. 2016, 16, 5815–5822

lithiation. In addition, the overall outward expansion of this nanotube is ~23%, which is smaller than ~31% for the nanotube with native oxides (Figure 1). Such a difference demonstrates the mechanical confinement effect of thick surface oxides on the outward expansion, which should be beneficial to mitigate mechanical degradation of SEIs on the outer surface of Si nanotubes.

To confirm the occurrence of inward expansion in nanotubes with thick oxides, we further studied the lithiation behavior of an *a*-Si nanotube with 4 and 6.5 nm SiO_x on the inner and outer surfaces, respectively (denoted as 4||6.5 nm SiO_x/Si/SiO_x nanotube), as shown in Figure 4g–i. Similar to the nanotube with native oxides (Figures 1 and 2) and the 3||4 nm nanotube (Figure 4b–f), lithiation of the 4||6.5 nm nanotube proceeded along the same reaction pathway, i.e., the sandwich lithiation mechanism and two-stage lithiation process (Figure S4). It is noted that the values of d_2 for 3||4 nm and 4||6.5 nm nanotubes were similar before lithiation; however, after full lithiation, d_2 decreased from 226 to 212 nm for the 3||4 nm nanotube (Figure 4c–f), but from 225 to 199 nm for the 4||6.5 nm nanotube (Figure 4g–i). The overall outward expansion of the 4||6.5 nm nanotube is ~19%, smaller than ~23% for the 3||4 nm nanotube (Figure 4b–f) and ~31% for the nanotube with native oxides (Figure 1). These results suggest that a more inward expansion occurred in nanotube with thicker SiO_x on the outer surface. Evidently, the volume expansion mode of *a*-Si nanotubes can be effectively changed by varying the thickness of surface coatings.

Previously, lithiation of Si nanotubes with an only outer SiO_x coating has been studied by ex situ experiments and simulations,[9,19] in which lithiation-induced outward expansion at the outer surface of Si nanotubes was claimed to be completely confined as the thickness of surface SiO_x increased. However, continual confinement was not observed during the lithiation of SiO_x/Si/SiO_x nanotubes studied here, as shown in Figure 5. In this case, the *a*-Si nanotube has 6.5 and 9 nm SiO_x layers on the inner and outer surfaces, respectively (denoted as 6.5||9 nm SiO_x/Si/SiO_x nanotube, Figure 5b). During in situ experiment, a high voltage (~20 V) had to be applied to initiate the lithiation, indicating that the thicker SiO_x coating becomes less conductive to electrons and/or Li ions. During lithiation, the outer SiO_x layer was first lithiated, accompanied by a thickness increase from 9 to 12 nm (Figure 5d). This process led to an outward expansion at the outer surface of this nanotube. Finally, concurrent lithiation occurred in both the outer and inner SiO_x layers, and their thicknesses reached 14 and 10 nm respectively after full lithiation (Figure 5c); meanwhile, a sandwich structure formed during the first-stage lithiation of the *a*-Si layer, which was followed by the second-stage lithiation of the *a*-Li_xSi phase, resulting in a total volume expansion of ~220% for *a*-Si (Figure 5e–f and Figure S5). After full lithiation, the diameters d_1, d_2, d_3, and d_4 changed to 175, 195, 278, and 305 nm, respectively, as opposed to 187, 202, 231, and 249 nm before lithiation. Hence a limited inward expansion occurred at the inner surface after lithiation of the 6.5||9 nm nanotube (Figure 5a,f). Figure 5g shows the modeling results of both the outer and inner diameters of the SiO_x/Si/SiO_x nanotube as a function of reduced time t^*, which are in close agreement with the experimental measurements (symbols). Moreover, the overall outward expansion of this nanotube is ~22%, which is similar to ~23% for the 3||4 nm nanotube but higher than ~19% for 4||6.5 nm nanotubes. These results imply that the inner SiO_x layer of SiO_x/Si/SiO_x nanotube can serve as a mechanical barrier to hinder inward expansion of the *a*-Si layer. The hindrance effect increases significantly with the thickness of the inner SiO_x layer. Thus, inner SiO_x layer should be minimized during fabrication, so as to enable an effective mechanical confinement from the SiO_x coating at the outer surface of nanotube. In our experiments of thermal oxidation, it was hard to prevent oxidation at the inner surface of *a*-Si nanotubes, since surface oxides grown concurrently at both their inner and outer surfaces.

To better understand the confinement effect of the outer SiO_x layer on lithiation of *a*-Si nanotubes, percentage contributions of inward and outward expansions of *a*-Si layer to the total volume of the fully lithiated *a*-Li_xSi alloy were further calculated based on the measured diameter changes after lithiation (Figure 5h). The oxide layers were excluded from this calculation. After lithiation, the contribution of outward expansion to the total volume can be calculated by $[(d_3^F/2)^2 - (d_3^I/2)^2]/[(d_3^F/2)^2 - (d_2^F/2)^2] \times 100\%$, and the contribution of inward expansion by $[(d_2^I/2)^2 - (d_2^F/2)^2]/[(d_3^F/2)^2 - (d_2^F/2)^2] \times 100\%$, where d_2^I and d_3^I respectively denote the values of d_2 and d_3 before lithiation, d_2^F and d_3^F after full lithiation; while the volumetric contribution from the initial *a*-Si layer is nearly a constant, with a theoretical value of 27% ($[V_{a\text{-Si}}/V_{Li_{15}Si_4}] \times 100\%$, where $V_{a\text{-Si}}$ and $V_{Li_{15}Si_4}$ are the volumes of *a*-Si and $Li_{15}Si_4$ phase, respectively). Figure 5h shows that the confinement effect on outward expansion (represented by the decreasing red curve and increasing black curve) can increase markedly with the increasing thickness of the outer SiO_x layer, and the maximum confinement is achieved in *a*-Si nanotubes with 6.5 nm outer SiO_x layer. However, a transition occurs as the thickness of outer SiO_x layer further increases, due to the increasing hindrance effect of the thicker inner SiO_x layer. Moreover, these results indicate that a more inward expansion at the inner surface could be achieved in each case if there was no SiO_x on the inner surface. Our quantitative calculation (Figure 5g) demonstrates that the lithiated thick SiO_x coatings can effectively impose mechanical constraints so as to reduce the outward expansion at the outer surface and correspondingly promote the inward expansion at the inner surface in lithiated SiO_x/Si/SiO_x nanotubes.

To summarize, our in situ TEM experiments have revealed the detailed lithiation behavior of individual *a*-Si nanotubes with different thicknesses of surface oxide layers. The real-time high-resolution imaging enables a precise measurement of the geometrical changes (with the nanometer resolution) during lithiation of *a*-Si nanotubes. Our results unambiguously show that outward expansion at the outer surface of lithiated *a*-Si nanotubes can be effectively confined by increasing the thickness of the outer SiO_x coating, while minimizing the thickness of the inner SiO_x coating can facilitate a more effective confinement by the outer SiO_x coating. Moreover, a high mechanical stability of lithiated SiO_x (i.e., no cracking after full lithiation) could avoid the repeated growth of SEI layers, thereby enhancing the cycle performance of Si nanotube electrodes. However, a more systematic study needs to be conducted by considering the effects of nanotube diameter and thicknesses of SiO_x coating and *a*-Si layer. Revealing such a mechanical confinement effect has practical implications for stabilizing SEIs and other types of coatings on the nanotube surface, in order to mitigate the mechanical degradation and associated capacity fade in LIBs.

DOI: 10.1021/acs.nanolett.6b02581
Nano Lett. 2016, 16, 5815–5822

Moreover, our in situ experimental and modeling results provide insights for the design of Si-based hollow anodes as follows. First, the lithiation-induced volume expansion (i.e., outward expansion at the outer surface) and resultant mechanical degradation of Si-based anodes can hardly be alleviated fully in hollow structures. This has been demonstrated by the lithiation behavior of *a*-Si nanotubes in Figures 1−2 as well as porous Si nanowire and nanoparticle in Figure S1. Second, for hollow structures with the active surface coatings, such as SiO_2,[9,16−21] Al_2O_3,[22] and carbon,[13,15,24] the lithiation-induced outward expansion cannot be fully constrained due to the fact that lithiation of the active surface coatings usually occurs before that of active Si, thereby resulting in outward expansion (Figures 4−5). This is in contrast to the earlier results from ex situ experiments and simulations, which claimed that the outward expansion of Si nanotubes were fully confined by the active surface coatings.[9,19] On the other hand, for hollow structures with the inactive surface coatings (e.g., metals[34]), outward expansion at the outer surface could be effectively suppressed due to the mechanical confinement of the surface coating that is thick enough. However, the use of thick inactive coatings would reduce the specific Li storage capacity of the electrode. Third, the surface coatings such as thermal oxides do not alter the lithiation mode of *a*-Si anodes as well as the resultant total volume expansion after full lithiation. For all of *a*-Si nanotubes studied here, their lithiation mechanisms were not affected by surface coatings. Finally, since SiO_x has poor conductivity and low capacity compared to Si,[35] a systematic study on the thickness effects of SiO_x is necessary for Si nanotube-based anodes in full battery cells, in order to determine the optimal combination of high capacity and mechanical stability. In addition, our chemomechanical modeling, in conjunction with in situ TEM experiments, also reveals the critical role of anisotropy of lithiation-induced chemical strains in the geometrical changes of lithiated Si. Overall, this work not only provides new insights into the degradation of nanotube anodes with or without surface coatings but also sheds light on the optimal design of novel hollow structures for high performance lithium-ion batteries.

■ ASSOCIATED CONTENT

Supporting Information

The Supporting Information is available free of charge on the ACS Publications website at DOI: 10.1021/acs.nanolett.6b02581.

Experimental and simulation methods and supporting figures (PDF)

■ AUTHOR INFORMATION

Corresponding Authors

*E-mail: (C.W.) chongmin.wang@pnnl.gov.
*E-mail: (J.W.) Jiangwei_Wang@zju.edu.cn.
*E-mail: (S.X.M.) sxm2@pitt.edu.

Author Contributions

▽J.W., H.L., and Y.L. contributed equally to this work.

Notes

The authors declare no competing financial interest.

■ ACKNOWLEDGMENTS

T.Z. acknowledges support by the NSF Grant CMMI 1100205 and DMR 1410936. J.W. acknowledges the support of the Chinese 1000-Youth-Talent Plan. H.L. acknowledges financial support from the China Scholarship Council. Work for PNNL is supported by the Assistant Secretary for Energy Efficiency and Renewable Energy, Office of Vehicle Technologies of the U.S. Department of Energy under Contract No. DE-AC02-05CH11231, Subcontract No. 6951379 under the advanced Battery Materials Research (BMR) program. Part of the work was conducted in the William R. Wiley Environmental Molecular Sciences Laboratory (EMSL), a national scientific user facility sponsored by DOE's Office of Biological and Environmental Research and located at PNNL. PNNL is operated by Battelle for the DOE under Contract DE-AC05-76RLO1830.

■ REFERENCES

(1) McDowell, M. T.; Lee, S. W.; Nix, W. D.; Cui, Y. *Adv. Mater.* **2013**, *25*, 4966−4985.
(2) Liu, X. H.; Zheng, H.; Zhong, L.; Huang, S.; Karki, K.; Zhang, L. Q.; Liu, Y.; Kushima, A.; Liang, W. T.; Wang, J. W.; Cho, J.-H.; Epstein, E.; Dayeh, S. A.; Picraux, S. T.; Zhu, T.; Li, J.; Sullivan, J. P.; Cumings, J.; Wang, C.; Mao, S. X.; Ye, Z. Z.; Zhang, S.; Huang, J. Y. *Nano Lett.* **2011**, *11*, 3312−3318.
(3) Liu, X. H.; Wang, J. W.; Huang, S.; Fan, F.; Huang, X.; Liu, Y.; Krylyuk, S.; Yoo, J.; Dayeh, S. A.; Davydov, A. V. *Nat. Nanotechnol.* **2012**, *7*, 749−756.
(4) Wang, X.; Fan, F.; Wang, J.; Wang, H.; Tao, S.; Yang, A.; Liu, Y.; Beng Chew, H.; Mao, S. X.; Zhu, T.; Xia, S. *Nat. Commun.* **2015**, *6*, 8417.
(5) Liu, X. H.; Liu, Y.; Kushima, A.; Zhang, S.; Zhu, T.; Li, J.; Huang, J. Y. *Adv. Energy Mater.* **2012**, *2*, 722−741.
(6) Kim, H.; Lee, E.-J.; Sun, Y.-K. *Mater. Today* **2014**, *17*, 285−297.
(7) Su, X.; Wu, Q.; Li, J.; Xiao, X.; Lott, A.; Lu, W.; Sheldon, B. W.; Wu, J. *Adv. Energy Mater.* **2014**, *4*, 1300882.
(8) Kim, H.; Han, B.; Choo, J.; Cho, J. *Angew. Chem., Int. Ed.* **2008**, *47*, 10151−10154.
(9) Wu, H.; Chan, G.; Choi, J. W.; Ryu, I.; Yao, Y.; McDowell, M. T.; Lee, S. W.; Jackson, A.; Yang, Y.; Hu, L.; Cui, Y. *Nat. Nanotechnol.* **2012**, *7*, 310−315.
(10) Sun, C.-F.; Karki, K.; Jia, Z.; Liao, H.; Zhang, Y.; Li, T.; Qi, Y.; Cumings, J.; Rubloff, G. W.; Wang, Y. *ACS Nano* **2013**, *7*, 2717−2724.
(11) Wang, J. W.; Liu, X. H.; Zhao, K.; Palmer, A.; Patten, E.; Burton, D.; Mao, S. X.; Suo, Z.; Huang, J. Y. *ACS Nano* **2012**, *6*, 9158−9167.
(12) Wang, C.-M.; Li, X.; Wang, Z.; Xu, W.; Liu, J.; Gao, F.; Kovarik, L.; Zhang, J.-G.; Howe, J.; Burton, D. J.; Liu, Z.; Xiao, X.; Thevuthasan, S.; Baer, D. R. *Nano Lett.* **2012**, *12*, 1624−1632.
(13) Gu, M.; Li, Y.; Li, X.; Hu, S.; Zhang, X.; Xu, W.; Thevuthasan, S.; Baer, D. R.; Zhang, J.-G.; Liu, J.; Wang, C. *ACS Nano* **2012**, *6*, 8439−8447.
(14) Zhao, J.; Lee, H.-W.; Sun, J.; Yan, K.; Liu, Y.; Liu, W.; Lu, Z.; Lin, D.; Zhou, G.; Cui, Y. *Proc. Natl. Acad. Sci. U. S. A.* **2016**, *113*, 7408−7413.
(15) Liu, J.; Li, N.; Goodman, M. D.; Zhang, H. G.; Epstein, E. S.; Huang, B.; Pan, Z.; Kim, J.; Choi, J. H.; Huang, X.; Liu, J.; Hsia, K. J.; Dillon, S. J.; Braun, P. V. *ACS Nano* **2015**, *9*, 1985−1994.
(16) Hassan, F. M.; Chabot, V.; Elsayed, A. R.; Xiao, X.; Chen, Z. *Nano Lett.* **2014**, *14*, 277−283.
(17) McDowell, M. T.; Lee, S. W.; Ryu, I.; Wu, H.; Nix, W. D.; Choi, J. W.; Cui, Y. *Nano Lett.* **2011**, *11*, 4018−4025.
(18) Sim, S.; Oh, P.; Park, S.; Cho, J. *Adv. Mater.* **2013**, *25*, 4498−4503.
(19) Xia, F.; Kim, S. B.; Cheng, H.; Lee, J. M.; Song, T.; Huang, Y.; Rogers, J. A.; Paik, U.; Park, W. I. *Nano Lett.* **2013**, *13*, 3340−3346.
(20) Yoo, H.; Lee, J.-I.; Kim, H.; Lee, J.-P.; Cho, J.; Park, S. *Nano Lett.* **2011**, *11*, 4324−4328.
(21) Yu, B.-C.; Hwa, Y.; Park, C.-M.; Kim, J.-H.; Sohn, H.-J. *RSC Adv.* **2013**, *3*, 9408−9413.
(22) Ye, J. C.; An, Y. H.; Heo, T. W.; Biener, M. M.; Nikolic, R. J.; Tang, M.; Jiang, H.; Wang, Y. M. *J. Power Sources* **2014**, *248*, 447−456.

DOI: 10.1021/acs.nanolett.6b02581
Nano Lett. 2016, 16, 5815−5822

(23) Lotfabad, E. M.; Kalisvaart, P.; Cui, K.; Kohandehghan, A.; Kupsta, M.; Olsen, B.; Mitlin, D. *Phys. Chem. Chem. Phys.* **2013**, *15*, 13646−13657.
(24) Jung, Y. S.; Lee, K. T.; Oh, S. M. *Electrochim. Acta* **2007**, *52*, 7061−7067.
(25) Ge, M.; Lu, Y.; Ercius, P.; Rong, J.; Fang, X.; Mecklenburg, M.; Zhou, C. *Nano Lett.* **2014**, *14*, 261−268.
(26) Ge, M.; Fang, X.; Rong, J.; Zhou, C. *Nanotechnology* **2013**, *24*, 422001.
(27) Wang, J. W.; He, Y.; Fan, F.; Liu, X. H.; Xia, S.; Liu, Y.; Harris, C. T.; Li, H.; Huang, J. Y.; Mao, S. X.; Zhu, T. *Nano Lett.* **2013**, *13*, 709−715.
(28) Huang, S.; Zhu, T. *J. Power Sources* **2011**, *196*, 3664−3668.
(29) Obrovac, M. N.; Christensen, L.; Le, D. B.; Dahn, J. R. *J. Electrochem. Soc.* **2007**, *154*, A849.
(30) Hong, W. *Extreme Mechanics Letters* **2015**, *2*, 46−51.
(31) Hsueh, C.-H.; Evans, A. G. *J. Appl. Phys.* **1983**, *54*, 6672−6686.
(32) Huang, S.; Fan, F.; Li, J.; Zhang, S.; Zhu, T. *Acta Mater.* **2013**, *61*, 4354−4364.
(33) Liang, W.; Yang, H.; Fan, F.; Liu, Y.; Liu, X. H.; Huang, J. Y.; Zhu, T.; Zhang, S. *ACS Nano* **2013**, *7*, 3427−3433.
(34) Karki, K.; Zhu, Y.; Liu, Y.; Sun, C.-F.; Hu, L.; Wang, Y.; Wang, C.; Cumings, J. *ACS Nano* **2013**, *7*, 8295−8302.
(35) Favors, Z.; Wang, W.; Bay, H. H.; George, A.; Ozkan, M.; Ozkan, C. S. *Sci. Rep.* **2014**, *4*, 4605.

DOI: 10.1021/acs.nanolett.6b02581
Nano Lett. 2016, 16, 5815−5822